

# Measurement of Mandibles with Microfocus X-ray Computerized Tomography and Compact Computerized Tomography for Dental Use

Munetaka Naitoh, DDS, PhD<sup>1</sup>/Akitoshi Katsumata, DDS, PhD<sup>2</sup>/Shogo Mitsuya, DDS<sup>3</sup>/  
Hiromasa Kamemoto, DDS, PhD<sup>4</sup>/Eiichiro Arijii, DDS, PhD<sup>5</sup>

**Purpose:** The trabecular bone patterns in jaws and tooth structure were analyzed using microfocus x-ray computerized tomography (micro-CT), and the usefulness of this method was reported. This study was performed to clarify the accuracy of micro-CT and to determine whether micro-CT could replace bone slice segments as a means for assessment of the accuracy of medical radiography units. In addition, the accuracy of compact CT for dental use (compact CT) was evaluated using the same method.

**Materials and Methods:** Three dried hemimandibles were used in this study. Images of mandibular interdental alveolar bone in the premolar and molar regions were obtained using micro-CT and compact CT. Measurement of the mandibular shape at 6 sites using micro-CT images and at 4 sites using compact CT images was performed, and then the values of the micro-CT and compact CT were compared with those of bone slice segments. **Results:** The accuracy of mandibular measurement and the ratios of agreement for micro-CT were significantly higher than those for compact CT. Moreover, the coefficient of correlation of the rate of trabecular bone between compact CT images and bone slice segment images was 0.916. **Discussion:** The significant difference in mandibular measurement between micro-CT and compact CT was considered to be related to pixel size. **Conclusion:** Micro-CT can replace bone slice segments for assessment of the accuracy of medical radiography units. In addition, compact CT can be used for imaging diagnosis in dental implant treatment. It is suggested that the ratio of trabecular bone could be used to evaluate the bone density. *INT J ORAL MAXILLOFAC IMPLANTS* 2004;19:239–246

**Key words:** biomedical technology assessment, compact computerized tomography, dental radiography, microfocus x-ray computerized tomography, trabecular bone patterns

Recently, microfocus x-ray computerized tomography (micro-CT) has emerged as a method for the nondestructive and detailed assessment of trabec-

ular bone patterns and tooth structure, and its usefulness has been reported.<sup>1–6</sup> Ide reported that the trabecular bone of mandibles appears to have a more platelike shape, rather than a rodlike shape, as determined by 3-dimensional observations with micro-CT.<sup>4</sup> In addition, Uchiyama and coworkers reported that there were significant correlations ( $0.95 \geq r \geq 0.79$ ) between micro-CT images and conventional histomorphometry of the bone volume, trabecular thickness, trabecular number, and trabecular separation of iliac bone biopsies.<sup>1</sup> However, the accuracy of the measurement of the shape of the mandible by micro-CT has not been evaluated.

In imaging diagnosis for osseointegrated dental implant treatment, cross-sectional images in the buccolingual direction delivered by conventional x-ray tomography or by CT are necessary.<sup>7–9</sup> Recently, compact CT for dental use (compact CT) was developed and will likely be used for dental implant treatment.<sup>10,11</sup> Accurate measurement of images using

<sup>1</sup>Associate Professor, Department of Oral and Maxillofacial Radiology, School of Dentistry, Aichi-Gakuin University, Nagoya, Japan; Chief of Oral Implant Clinic, Dental Hospital, Aichi-Gakuin University, Nagoya, Japan.

<sup>2</sup>Associate Professor, Department of Oral Radiology, Asahi University School of Dentistry, Gifu, Japan.

<sup>3</sup>Researcher, Department of Oral and Maxillofacial Radiology, School of Dentistry, Aichi-Gakuin University, Nagoya, Japan.

<sup>4</sup>Part-time Instructor, Department of Oral Radiology, Asahi University School of Dentistry, Gifu, Japan.

<sup>5</sup>Professor and Chairman, Department of Oral and Maxillofacial Radiology, School of Dentistry, Aichi-Gakuin University, Nagoya, Japan.

**Correspondence to:** Dr Munetaka Naitoh, Department of Oral and Maxillofacial Radiology, School of Dentistry, Aichi-Gakuin University, 2-11, Suemori-Dori, Chikusa-Ku, Nagoya 464-8651, Japan. Fax: +81-527592165. E-mail: mune@dpc.aichi-gakuin.ac.jp

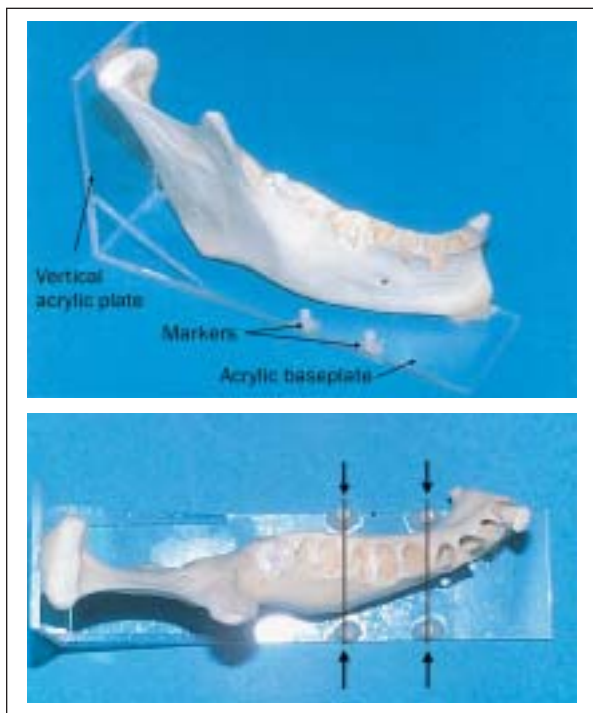


**Fig 1** (Top) Dried hemimandible. (Bottom) The premolar and molar regions were investigated (arrows).

these techniques has usually been assessed with bone slice segments.<sup>12-16</sup> The findings obtained on CT images have been compared with bone slice segments, which are regarded as a gold standard.

The present study was performed to clarify the accuracy of micro-CT and to determine whether micro-CT could replace bone slice segments for an assessment of the accuracy of medical radiography units. If micro-CT images of mandibles are obtained once, the same mandibles could be used as test objects for medical radiography units without bone slice segments, thus simplifying the assessment of accuracy between medical radiography units. The reconstructed thickness of micro-CT images could duplicate the same slice thickness of a medical radiography unit by piling up thin slices of micro-CT images. Therefore, it might be possible to continuously evaluate mandibles without any loss of the section. In addition, this study was intended to help to clarify the accuracy of measurements of the shape of mandibles using compact CT in the same way as for the micro-CT study.

## MATERIALS AND METHODS

### Dried Mandibles

Three dried human hemimandibles from which the premolars and the molars had been extracted were

used in this investigation. Two pieces of acrylic resin plate were fixed at a right angle, and then the mandibles were set on an acrylic resin baseplate (Fig 1). Two of the 3 hemimandibles were positioned to nearly parallel the interdental alveolar bone between the first and second premolars and between the first and second molars. The third hemimandible was positioned nearly parallel to the interdental alveolar bone between the second premolar and first molar and between the first and second molars. Six regions were examined in the micro-CT study. In the compact CT study, 4 of the 6 regions were examined. The imaginary occlusal plane was set parallel to the acrylic resin baseplate, and the buccolingual direction of the interdental alveolar bone in these 6 regions was set parallel to the vertical acrylic resin plate. Markers (diameter: 2.7 mm, length: 5.3 mm) made from a light-curing resin (Z100; 3M Dental Products, St Paul, MN) were set at the outer portion of the 6 regions.

### Micro-CT

A series of images of the region from the first premolar to the second molar were obtained using a micro-CT unit (SMX-130CT; Shimadzu, Kyoto, Japan). The vertical acrylic resin plate was set on the stage. The exposure conditions were 47 kV and 67  $\mu$ A with a 40.96-mm field of view (FOV) and 0.152-mm thick slices with 0.152-mm intervals. The information from all slices was saved as 16-bit TIFF files and 1,024  $\times$  1,024 matrix data (1 pixel = 40  $\times$  40  $\mu$ m). The images were analyzed on a computer (Macintosh G3 266; Apple Computer, Cupertino, CA) and image processes were performed as follows. First, using image-analyzing software (NIH Image, version 1.62; National Institutes of Health, Bethesda, MD), 15 continuous slices (thickness: 2.28 mm) were selected from both the premolar and molar regions. Second, the 15 slices were displayed as stacked images, and the average image was obtained by averaging the pixel values in 15 slices (Fig 2).

### Compact CT

A series of images in the premolar and molar regions were obtained using a compact CT unit (3DX; Morita, Kyoto, Japan) (Fig 3a). The vertical acrylic resin plate was set on the stage. The exposure conditions were 80 kV and 3 mA with a 0.5-mm copper filter. The images were reconstructed as 0.125-mm-thick slices with 0.125-mm intervals. The information from all coronal slices was saved as 8-bit TIFF files and 240  $\times$  320 matrix data (1 pixel = 0.125  $\times$  0.125 mm). Image processing was performed in the same way as for the micro-CT study.

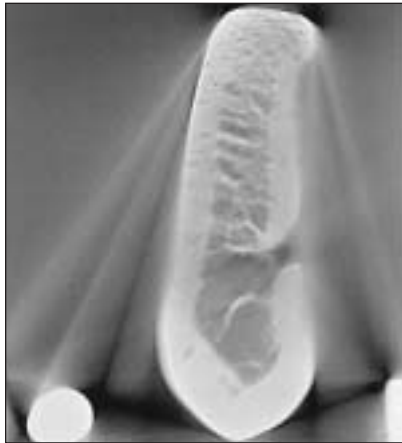


**Fig 2** Averaged micro-CT image from the premolar region. Fifteen continuous slices were selected in the premolar region, and an average image was obtained using imaging software.



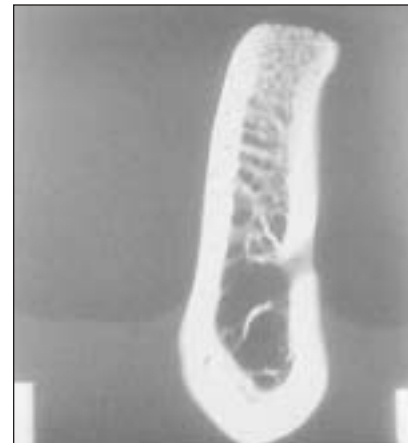
**Fig 3a** Compact CT unit (3DX; Morita, Kyoto, Japan).



**Fig 3b** Averaged compact CT image from the premolar region. Eighteen continuous slices were selected in the premolar region, and an average image was obtained using imaging software.

**Fig 4a** (Left) Bone slice segment from the premolar region.

**Fig 4b** (Right) Contact radiograph of the bone slice segment from the premolar region.



The average image was obtained by averaging the pixel values in 18 continuous slices (Fig 3b).

#### Bone Slice Segments

Bone slice segments in 6 regions, paralleling the vertical acrylic resin plate, were obtained using a micro-cutting machine (BS-300; Exakt Apparatebau, Hamburg, Germany) (Fig 4a). The thickness of bone slice segments was similar to the thickness of the micro-CT average images. The thickness of each bone slice segment was measured 5 times using a digital caliper (CD-S15; Mitutoyo, Tokyo, Japan). Then contact radiographs of bone slice segments were obtained using a medical radiography unit (R-20; Shimadzu) at exposure conditions of 40 kV and 25 mAs with a focus-film distance (FFD) of 100 cm and dental x-ray film (Insight; Eastman Kodak, Rochester, NY). The radiographs were converted to digital images using a charge-coupled device video camera (KY-

F55MD; Olympus, Tokyo, Japan) and a color image analyzer (SP500F; Olympus). The images were saved as 8-bit TIFF files and  $512 \times 512$  matrix data (1 pixel =  $75 \times 75 \mu\text{m}$ ) (Fig 4b).

#### Quantitative Evaluation

To determine the accuracy of micro-CT and compact CT, the measurements of the micro-CT images and compact CT images were compared with the measurements of the bone slice segments. At 6 points of cortical bone and 6 points of air surrounding the bone, the micro-CT images, compact CT images, and bone slice images were averaged using image-editing software (Photoshop, version 5.5; Adobe Systems, San Jose, CA) (Fig 5).

For the measurement of the hemimandibles, the following points were defined on the black and white binary images: the superior border (point of the alveolar crest) and the inferior border (point of

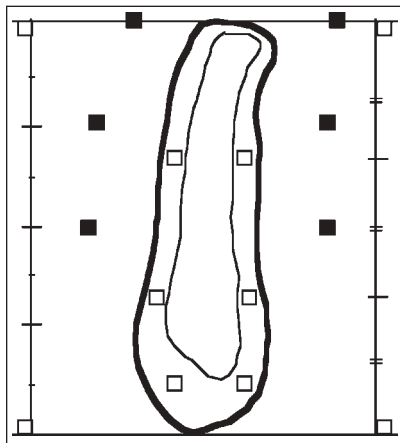


**Fig 5** Schematic drawing to obtain a black and white (2-value) image. The regions of interest (ROIs) for cortical bone (white squares) and for the air area (black squares) were designed to avoid artifacts.



**Fig 6a** Subtraction image between averaged micro-CT image and bone slice segment image in the premolar region. Areas of agreement are indicated by gray, and areas of disagreement are indicated by white or black.

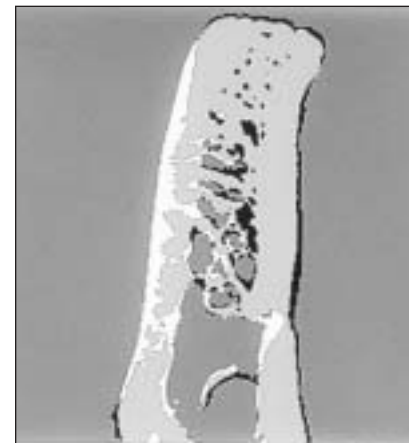


**Fig 6b** Subtraction image between averaged compact CT image and bone slice segment image in the premolar region. Areas of agreement are indicated by gray, and areas of disagreement are indicated by white or black.

inferior mandible) of the mandible paralleling the acrylic resin baseplate and the outer surface (buccal point and lingual point) of cortical plates perpendicular to the baseplate. Bone height, defined as the length from the alveolar crest to the inferior mandible perpendicular to the baseplate, and bone width, defined as the length between the buccal and lingual points paralleling the baseplate, were measured using the micro-CT average images, compact CT average images, and bone slice segment images. Then the thickness of cortical bone in the inferior mandible and at the buccal and lingual points was measured. The measurement values were compared using the following calculations.

$$\text{Difference} = (\text{M-CT or CCT}) - \text{BS}$$

$$\text{Mean difference} = \frac{\sum |(\text{M-CT or CCT}) - \text{BS}|}{\text{No. of measurements}}$$

Where M-CT is the measurement value from the micro-CT; CCT is the compact CT average image; and BS is the measurement value from the bone slice segment image.

Subsequently, the ratios of agreement in the mandible (bone and the interspace of trabecular bone patterns) were calculated between micro-CT average images and bone slice segment images and between compact CT average images and bone slice segment images using image-editing software (Photoshop). The black and white binary images of micro-CT average images, compact CT average images, and bone slice segment images were used.

The pixel size was standardized between micro-CT average images and bone slice segment images and between compact CT average images and bone slice segment images, and the number of pixels in the area of the mandible was quantified on each bone slice segment image. After micro-CT average images or compact CT average images were converted to black and white, micro-CT average images or compact CT average images were superimposed onto the bone slice segment images using the markers as guides (Figs 6a and 6b). The “agreeing” pixels appeared gray and the “disagreeing” pixels appeared white or black. Then, the number of pixels in the gray areas (the number of pixels in agreement) was measured, and the ratios of agreement in bone and the interspace of the trabecular bone patterns between micro-CT average images and bone slice segment images and between compact CT average images and bone slice segment images were calculated using the following equation:

$$\text{RA} (\%) = \frac{\text{No. of pixels in agreement area}}{\text{No. of pixels in the mandibular area}} \times 100$$

In addition, the trabecular bone patterns were quantitatively compared between compact CT average images and bone slice segment images. In each black and white binary image, regions of interest (ROI) were set for the whole sample, for the superior half, and for the inferior half in the cancellous bone. The ratio of the trabecular bone was calculated using the following equation:

**Table 1 Measurements of the Hemimandibles**

Method	Differences in mandibular shape (mm)			Differences in cortical bone thickness (mm)		
	Mean	SD	Range	Mean	SD	Range
Micro-CT	0.08*	0.08	-0.23 to 0.08	0.19	0.13	-0.45 to 0.38
Compact CT	0.42*	0.18	0.28 to 0.67	0.18	0.16	0.00 to 0.38

\*P < .05.

$$RTB (\%) = \frac{\text{No. of pixels in trabecular bone}}{\text{No. of pixels in the ROI}} \times 100$$

The correlation between the findings was analyzed with software (StatView version 4.0; Abacus Concepts, Cary, NC).

In the compact CT images, the height was 30 mm and an artifact was observed in the inferior area. Since the distance from the alveolar crest to the inferior border in the premolar region was greater than 30 mm, the measurement of height was performed in 2 molar regions and the subtraction was performed into the range of 25 mm from the alveolar crest.

**Statistical Analysis**

The differences between the obtained values were evaluated using the Mann-Whitney U test. The testing was considered significant if P < .05.

**RESULTS**

**Bone Slice Segments**

The thickness of bone slice segments ranged from 2.21 to 2.34 mm in 6 regions; the mean was 2.27 mm. As to shape, the mean and standard deviation (SD) of the distance from the alveolar crest to the inferior border of the mandible was 28.2 ± 2.0 mm. The mean (± SD) of the length between the outer surfaces of the cortical plates was 13.2 ± 2.0 mm. The mean width of the cortical bone (± SD) was 2.4 mm ± 1.1 mm.

**Micro-CT**

For the shape, the mean and SD of the length from the alveolar crest to the inferior border of the mandible was 28.2 ± 2.0 mm. The mean and SD of the length between the outer surfaces of the cortical plates was 13.1 ± 2.0 mm. The mean difference was 0.08 mm (from -0.23 to 0.08 mm). For the width of cortical bone, the mean (± SD) was 2.4 ± 1.0 mm, and the mean difference was 0.19 mm (from -0.45 to

**Table 2 Ratios of Agreement Between Micro-CT Images and Bone Slice Segment Images and Between Compact CT Images and Bone Slice Segment Images**

Sample no.	Micro-CT versus bone slice segments	Compact CT versus bone slice segments
1	85.1%	81.8%
2	87.6%	74.3%
3	83.2%	74.8%
4	86.1%	70.6%
5	81.1%	N/A
6	87.3%	N/A
Mean	85.1% *	75.4% *
SD	2.5%	4.7%

\*P < .05.

0.38 mm) (Table 1). The ratios of agreement were from 81.1% to 87.6% in 6 regions, and the mean ratio of agreement was 85.1% (Table 2).

**Compact CT**

For the shape, the mean (± SD) of the length from the alveolar crest to the inferior border of the mandible was 26.3 ± 0.2 mm in 2 molar regions. The mean (± SD) of the length between the outer surfaces of the cortical plates was 13.0 ± 1.8 mm in 4 regions. The mean difference was 0.42 mm (from 0.28 to 0.67 mm). With respect to the width of cortical bone, the mean (± SD) was 2.9 ± 0.9 mm, and the mean difference was 0.19 mm (from 0 to 0.38 mm) (Table 1). The ratios of agreement ranged from 70.6% to 81.8% in 4 regions, and the mean ratio was 75.4% (Table 2). The coefficient of correlation of the ratio of trabecular bone between compact CT average images and bone slice segment images was 0.916 (Fig 7).

**DISCUSSION**

The measurement accuracy of micro-CT has not been evaluated previously using bones. The method

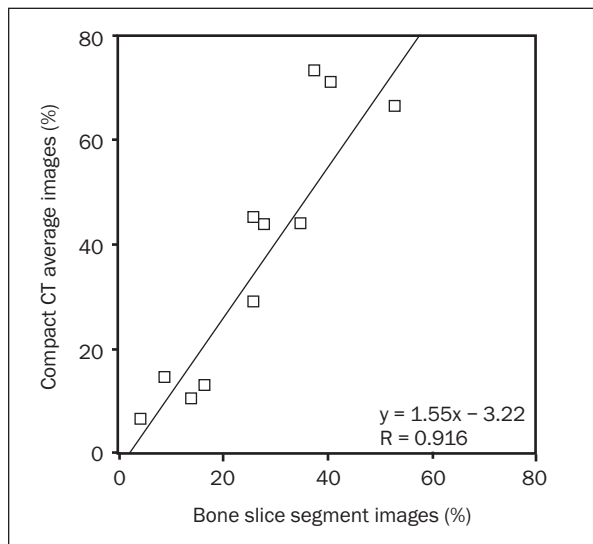


**Fig 7** The ratios of the trabecular bone between averaged compact CT images and bone slice segment images. Approximate straight line:  $y = 1.55x - 3.22$ .

typically employed to assess the measurement accuracy of medical radiography units<sup>12-16</sup> was used. The examination by micro-CT was performed before dividing bone slice segments. It is possible that bone slice segments can be performed by micro-CT; however, it was difficult to set bone slice segments exactly paralleling and over the stage of the micro-CT unit. Therefore, thin and continuous slices were obtained by micro-CT, and then the average image was determined using image-editing software. The study was designed so that the thickness of the average image was similar to the thickness of the bone slice segments. Small differences of some hundredths of millimeters were observed between the micro-CT average images and bone slice segments; however, these differences should not have affected the present investigation. The site of bone slice segments was set at the same site as the micro-CT and compact CT images using the resin markers, and the plane of bone slice segments was set in the same plane as the micro-CT and compact CT images using the vertical acrylic resin plate. The bone segments were not measured directly using a digital caliper, whereas the number of pixels was measured on black and white binary images of the contact radiograms. This method was assumed to be more quantitative.

The differences between the actual objects and medical CT images, considered one of the most accurate tomographic units, are to be approximately 0.1 mm in the horizontal direction, as assessed in previous studies using gutta-percha rectangles and a

rectangular parallel-piped phantom with hydroxyapatite.<sup>17,18</sup> In the present investigation, a significant difference in the accuracy of mandibular measurements was found between micro-CT and compact CT. For micro-CT, just 1.1 pixels differed in bone shape, which confirms the high measurement accuracy. For the ratios of agreement, a significant difference was found between micro-CT and compact CT. It was considered that this result was related to pixel size. The pixel size of the compact CT was  $125 \times 125 \mu\text{m}$ , and it has been reported that the resolution of micro-CT is  $10^2$  to  $10^3$  times greater than the current medical CT.<sup>19</sup> A comparison of the micro-CT (1 pixel =  $40 \times 40 \mu\text{m}$ ) and the medical CT at the authors' hospital (1 pixel =  $0.35 \times 0.35 \text{ mm}$ ), showed that the resolution of the micro-CT was  $10^2$  times greater. The resolution is lower for imaging diagnosis involved in dental implant treatment, since reformatted images have to be reconstructed using sequentially piled up axial CT images. However, with micro-CT, the objective planes of samples are obtained directly by setting the sample optimally on the stage, so the resolution of micro-CT images is ensured a definite value. The differences in the cortical thickness are slightly larger than those for shape. It has been suggested that the partial volume effect reported by Todd and coworkers<sup>13</sup> and the shape of the mandible are responsible.

The ratios of agreement in bone and the interspace of the trabecular bone patterns between micro-CT average images and bone slice segment images were relatively high. Uchiyama and coworkers<sup>1</sup> reported that the difference in correlation coefficients between the micro-CT image analysis and conventional histomorphometry could be caused by 3 factors: the resolution in micro-CT, the threshold value in micro-CT, and the shrinkage of tissue during cutting and histologic processing. The errors in the present result were probably caused by the loss of noncontinuous trabecular bone to surrounding bone. Resin embedding could cause artifacts in micro-CT, so the mandibles were not embedded. In addition, it has been reported that the width of mandibular trabecular bone was between 0.080 and 0.418 mm, with a mean of 0.191 mm (SD 0.054 mm).<sup>20</sup> Slices in micro-CT (0.152 mm) were slightly thick compared with thin trabecular bone. Moreover, small differences in the thickness were observed between micro-CT average images and bone slice segments.

In the present study, the measurement values of micro-CT average images were close to those of bone slice segments. Thus, it is proposed that micro-CT can replace bone slice segments for an assessment of

the accuracy of medical radiography units. In the compact CT study, the differences in mandibular measurement were similar to those of previous studies that used medical CT and tomography.<sup>13,17,21</sup> In addition, the coefficient of correlation of the ratio of trabecular bone was high; however, the inclination of the approximate straight line between compact CT average images and bone slice segment images was 1.55, not 1. It is suggested that the errors in these results were caused by the loss of trabecular bone contacting surrounding bone when performing a bone slice segment. CT, obtained as cross-sectional images, is capable of providing a numeric value (expressed in Hounsfield units) for the linear attenuation coefficient of a region of bone, which may provide a crude indication of bone density.<sup>9</sup> In contrast, the pixel value of an image obtained by compact CT is a relative value, not an absolute value like the Hounsfield unit. From the present results, it is proposed that compact CT can be used for imaging diagnosis in dental implant treatment, and bone density could be evaluated using the ratio of trabecular bone.

Further studies in regard to image quality, metal artifacts, and cost are needed to evaluate the clinical use of compact CT.

## CONCLUSIONS

Measurements of the mandibular shape using micro-CT images were made, and it was determined that micro-CT could replace bone slice segments for an assessment of the accuracy of medical radiography units. In addition, the accuracy of compact CT was clarified using the same method.

Images of interdental alveolar bone in the mandibular premolar and molar regions were obtained using a micro-CT unit and a compact CT unit. The micro-CT images and compact CT images were then compared with contact radiographs of bone slice segments. The measurements obtained from micro-CT images and compact CT images were similar to those obtained from bone slice segments.

The accuracy of mandibular measurement and the ratios of agreement for micro-CT were significantly higher than those for compact CT. Moreover, the coefficient of correlation of the ratio of trabecular bone between compact CT images and bone slice segment images was 0.916.

These results suggest that micro-CT can replace bone slice segments for an assessment of the accuracy of medical radiography units. Compact CT may be used for imaging diagnosis in dental implant treatment, and bone density may be evaluated using the ratio of trabecular bone.

## ACKNOWLEDGMENTS

We thank Mr M. Natsuhara, Mr M. Kataoka, and Mr T. Toshikura of the Shimadzu Corporation for their cooperation in performing the micro-CT imaging.

## REFERENCES

1. Uchiyama T, Tanizawa T, Muramatsu H, Endo N, Takahashi HE, Hara T. A morphometric comparison of trabecular structure of human ilium between micro-computed tomography and conventional histomorphometry. *Calcif Tissue Int* 1997;61:493-498.
2. Ito M, Nakamura T, Matsumoto T, Tsurusaki K, Hayashi K. Analysis of the trabecular microarchitecture of human iliac bone using microcomputed tomography in patients with hip arthrosis with or without vertebral fracture. *Bone* 1998;23:163-169.
3. Muller R, van Campenhout H, van Damme B, et al. Morphometric analysis of human bone biopsies: A quantitative structural comparison of histological sections and micro-computed tomography. *Bone* 1998;23:59-66.
4. Ide Y. Morphological changes of the mandible with loss of the teeth: Observation of the trabecular bone using micro-CT [in Japanese]. *Acta Anat Nippon* 2000;75:357-364.
5. Sennerby L, Wennerberg A, Pasop F. A new microtomographic technique for non-invasive evaluation of the bone structure around implants. *Clin Oral Implants Res* 2001;12:91-94.
6. Dowker SEP, Davis GR, Elliott JC. X-ray microtomography. *Oral Surg Oral Med Oral Pathol Oral Radiol Endod* 1997;83:510-516.
7. Hollender L. Radiographic examination of endosseous implants in the jaws. In: Worthington P, Brånemark P-I (eds). *Advanced Osseointegration Surgery: Applications in the Maxillofacial Region*. Chicago: Quintessence, 1992: 80-89.
8. Ekstubby A, Grondahl K, Grondahl H-G. The use of tomography for dental implant planning. *Dentomaxillofac Radiol* 1997;26:206-213.
9. Wyatt CCL, Pharoah MJ. Imaging techniques and image interpretation for dental implant treatment. *Int J Prosthodont* 1998;11:442-452.
10. Ito K, Gomi Y, Sato S, Arai Y, Shinoda K. Clinical application of a new compact CT system to assess 3-D images for the preoperative treatment planning of implants in the posterior mandible: A case report. *Clin Oral Implants Res* 2001;12:539-542.
11. Kobayashi K, Shimoda S, Yamamoto A. Assessment of limited cone beam CT for the preoperative examination of dental implant. Presented at the 5th World Congress for Oral Implantology, Japan Division, Tokyo, 30 Jun-2 Jul 2001.
12. Klinge B, Petersson A, Maly P. Location of the mandibular canal: Comparison of macroscopic findings, conventional radiography, and computed tomography. *Int J Oral Maxillofac Implants* 1989;4:327-332.
13. Todd AD, Gher ME, Quintero G, Richardson AC. Interpretation of linear and computed tomograms in the assessment of implant recipient sites. *J Periodontol* 1993;64:1243-1249.
14. Potter BJ, Shrout MK, Russell CM, Sharawy M. Implant site assessment using panoramic cross-sectional tomographic imaging. *Oral Surg Oral Med Oral Pathol Oral Radiol Endod* 1997;84:436-442.

15. Bou Serhal CB, Jacobs R, Persoons M, Hermans R, van Steenberghe D. The accuracy of spiral tomography to assess bone quantity for the preoperative planning of implants in the posterior maxilla. *Clin Oral Implants Res* 2000;11: 242–247.
16. Bou Serhal CB, van Steenberghe D, Quiryen M, Jacobs R. Localisation of the mandibular canal using conventional spiral tomography: A human cadaver study. *Clin Oral Implants Res* 2001;12:230–236.
17. Sonick M, Arahams J, Faiella RA. A comparison of the accuracy of periapical, panoramic, and computerized tomographic radiographs in locating the mandibular canal. *Int J Oral Maxillofac Implants* 1994;9:455–460.
18. Naitoh M, Takeuchi K, Kito M, et al. Measurement of edentulous alveolar process of the maxilla by reformatted CT images. *J Jpn Soc Oral Implantol* 1999;12:246–254.
19. Shibata T, Matsumoto S, Nagano T. Tomograms of arterial system of the human fetal auditory apparatus obtained by very-high-resolution microfocus X-ray CT and 3D reconstruction. *Acta Anat Nippon* 1999;74:545–553.
20. Monov G, Ulm C, Donath K, Tepper G, Watzek G. Histomorphometric study in the human mandible to assess atrophy-associated changes [abstract]. *Clin Oral Implants Res* 2002;13:xxviii.
21. Petrikowski CG, Pharoah MJ, Schmitt A. Presurgical radiographic assessment for implants. *J Prosthet Dent* 1989;61: 59–64.